Supplementary Figure S1

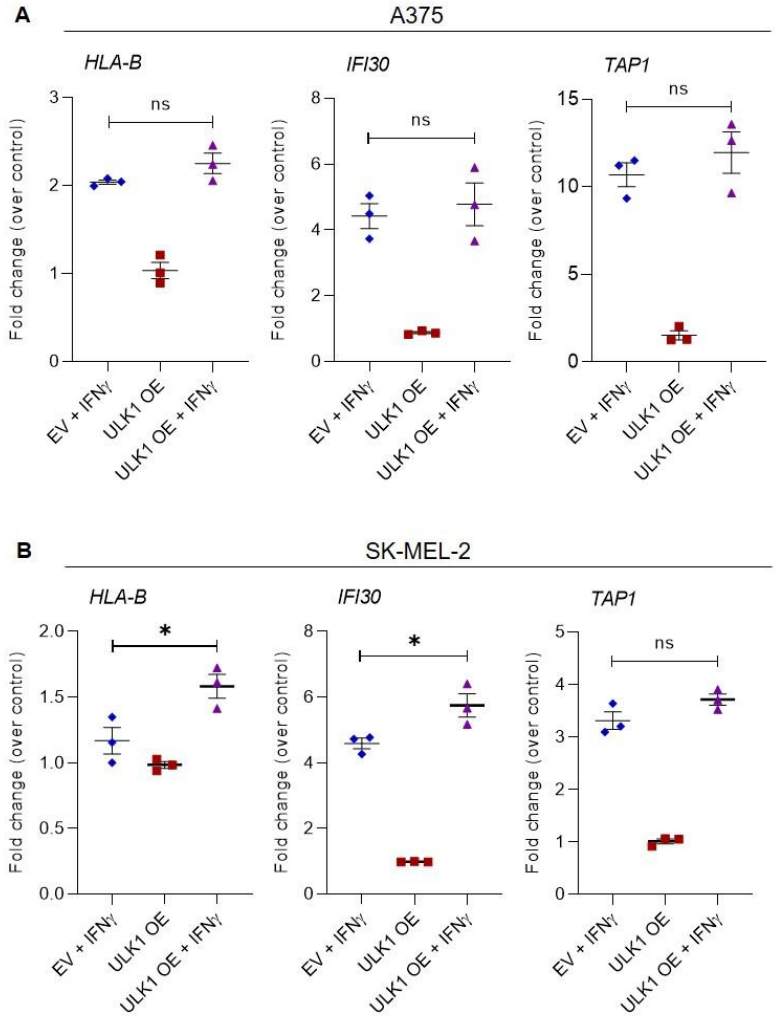

Supplementary Figure S1. **Overexpression of *ULK1* in melanoma cells has minor effects on transcription of IFNγ-induced immunostimulatory genes.** (A-B) (A) A375 and (B) SK-MEL-2 melanoma cells were transfected with either empty vector (EV) or ULK1 expression plasmid (ULK1 OE). The next day, transfected cells were either left untreated or were treated with IFNγ (2500 IU/mL) for 6 hours and then processed for qRT-PCR analysis. Scatter dot plots show fold change of mRNA expression for the indicated genes over untreated EV-transfected cells (control). Shown are means ± SEM from three independent experiments (the same shown in figure 1E for A375 cells and in figure 1F for SK-MEL-2 cells). Statistical analyses were performed using one-way ANOVA followed by Tukey's multiple comparisons test. *, $p < 0.05$, ns (not significant), $p > 0.05$.

Supplementary Figure S2

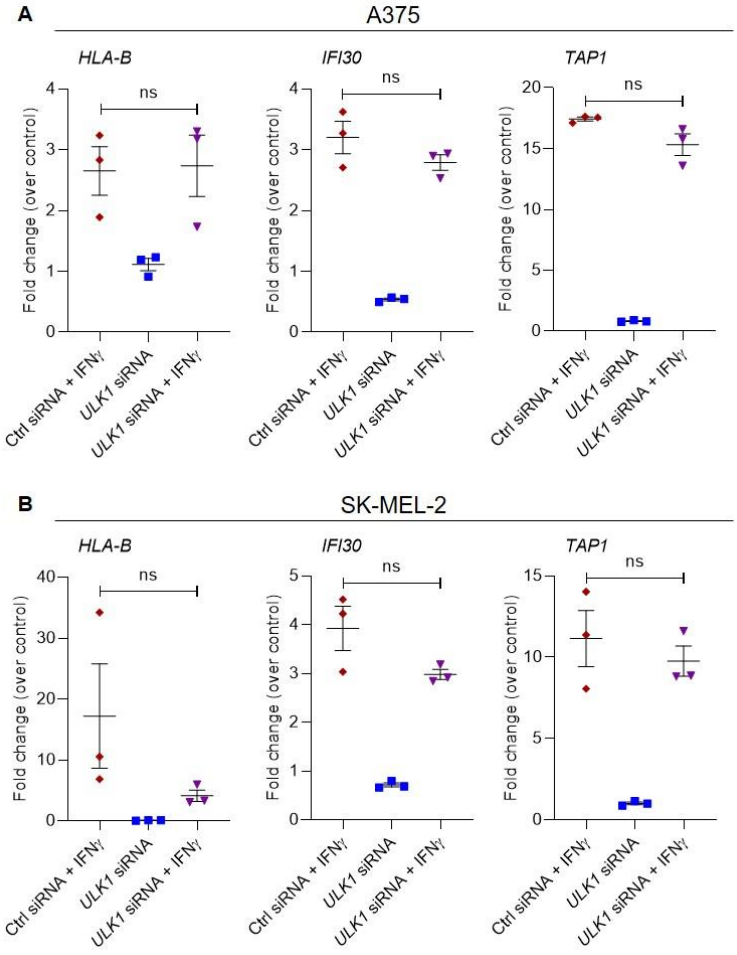

Supplementary Figure S2. Effects of gene targeted inhibition of *ULK1* in transcription of IFNγ-induced immunostimulatory genes in melanoma cells. (A-B) qRT-PCR analysis of *HLA-B*, *IFI30* and *TAP1* mRNA expression in control (Ctrl) siRNA or *ULK1* siRNA-transfected (A) A375 and (B) SK-MEL-2 melanoma cells, either left untreated or treated with IFNγ (2500 IU/mL) for 6 hours. Scatter dot plots, with means ± SEM from three independent experiments (same as shown in figure 2 A and B), show fold change of mRNA expression for each gene compared to Ctrl siRNA-transfected untreated cells (control) for each independent experiment. Statistical analyses were performed using one-way ANOVA followed by Tukey's multiple comparisons test. ns (not significant), $p > 0.05$.

Supplementary Figure S3

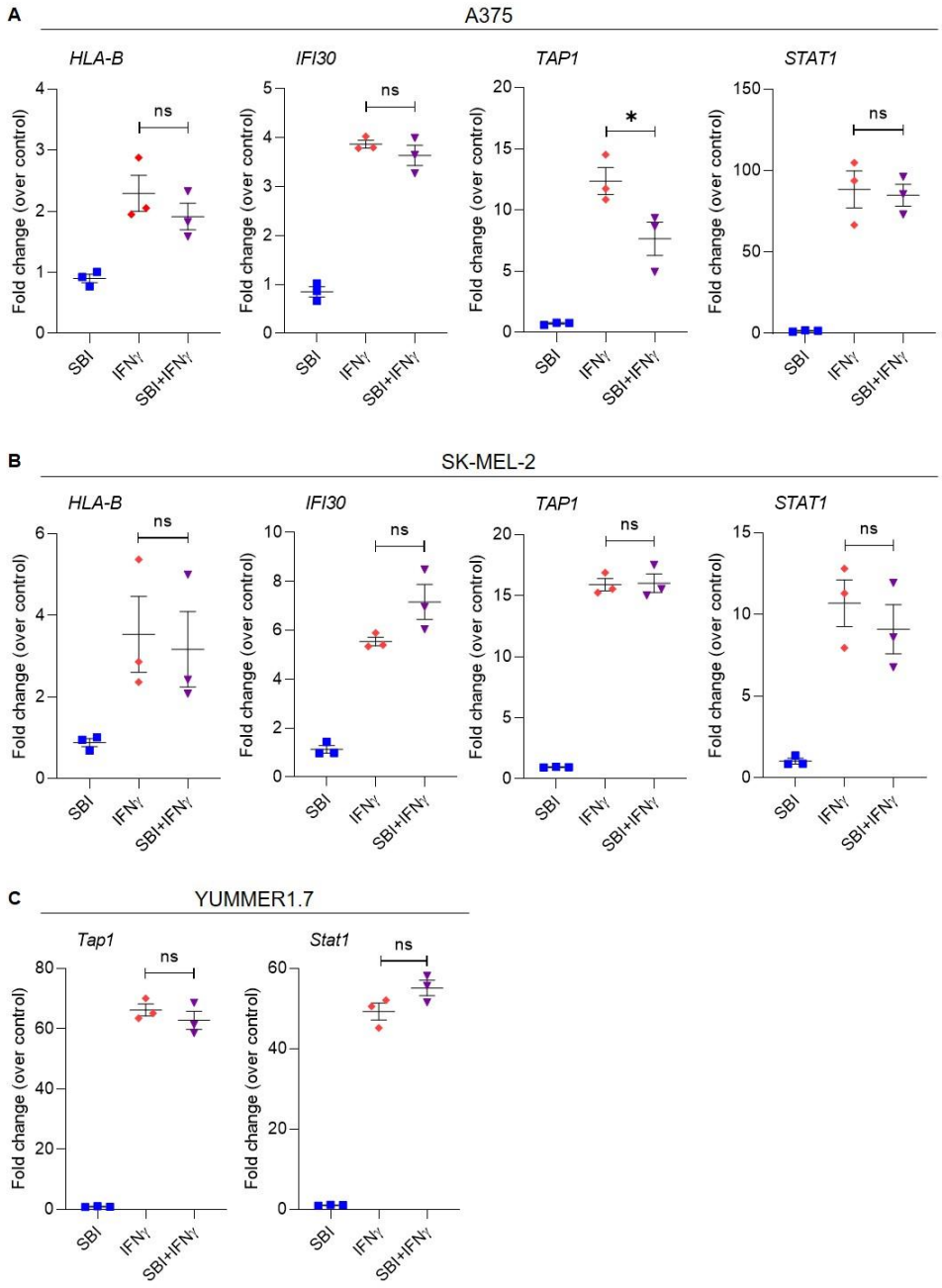

Supplementary Figure S3. Effects of drug-targeted inhibition of ULK1 in transcription of IFNγ-induced immunostimulatory genes in melanoma cells. (A-C) qRT-PCR analysis of *HLA-B*, *IFI30, TAP1* and *STAT1* mRNA expression in (A) A375 and (B) SK-MEL-2 and of *Tap1* and *Stat1* in (C) YUMMER1.7 cells treated with either vehicle (DMSO, control), the ULK kinase inhibitor SBI-0206965 (SBI) (10 μM), IFNγ (2500 IU/mL) or combination therapy with SBI-0206965 and IFNγ (SBI + IFNγ) for

6 hours. Scatter dot plots, with means ± SEM from three independent experiments (same as shown in figure 3 A-C, respectively), show fold change of mRNA expression for each gene compared to vehicle-treated cells (control) for each independent experiment. Statistical analyses were performed using one-way ANOVA followed by Tukey's multiple comparisons test. *, $p < 0.05$, ns (not significant), $p > 0.05$.

Supplementary Figure S4

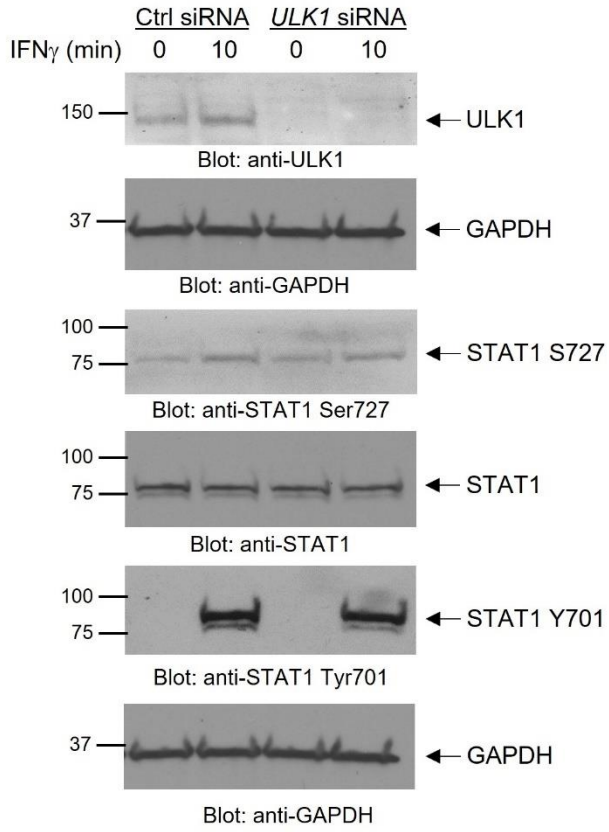

Supplementary Figure S4. Effects of siRNA-mediated knockdown of *ULK1* on IFNγ-induced STAT1 phosphorylation. Immunoblotting analysis of the indicated proteins in control (Ctrl) siRNA or *ULK1* siRNA-transfected A375 melanoma cells, either left untreated or treated with IFNγ (5000 IU/mL) for 10 minutes. Equal amounts of total cell lysates were ran in one gel to detect ULK1, GAPDH and STAT1 Ser727. The blot for STAT1 Ser727 was stripped, blocked, and reblotted to detect the levels of total STAT1 (four top blots shown). In parallel, equal amounts of the same total cell lysates were ran in another gel to detect STAT1 Tyr701 and GAPDH (two bottom blots shown). Immunoblots shown are representative of three experiments.

Supplementary Figure S5

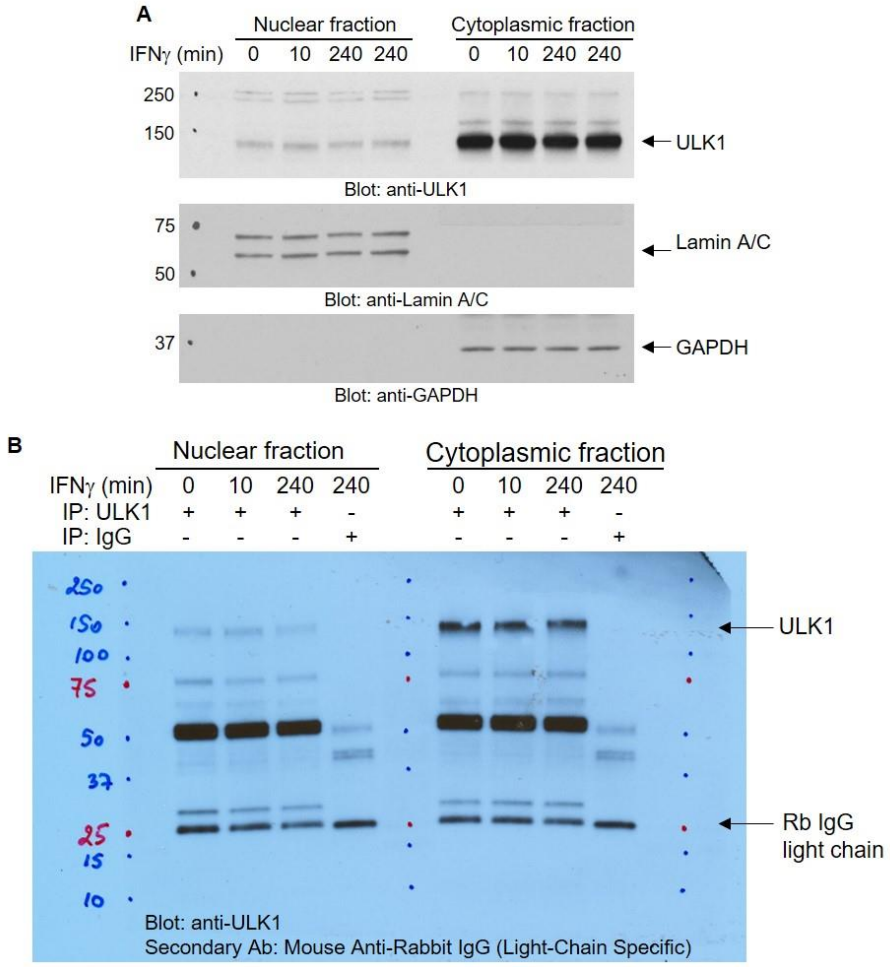

Supplementary Figure S5. Identification of putative cytoplasmic and nuclear ULK1 binding partners in melanoma cells upon IFNγ stimulation by mass spectrometry analysis. (A-B) A375 cells were either left untreated or were treated with IFNγ for 10 min (5000 IU/mL) or 4 hours (2500 IU/mL), followed by cytoplasmic and nuclear cell fractionation. (A) Equal amounts of nuclear and cytoplasmic protein lysates for each treatment condition were resolved by SDS-PAGE and immunoblotting analysis was performed for ULK1. Lamin A/C and GAPDH were used as loading control for the nuclear and cytoplasmic compartments, respectively. (B) ULK1-protein complexes were co-immunoprecipitated (IP) using an anti-ULK1 monoclonal specific antibody conjugated to sepharose beads for each compartment/treatment condition. As negative control, the same procedure was followed, but using a rabbit monoclonal IgG isotype control conjugated to sepharose beads instead of

the anti-ULK1 antibody for the 4 hours (240 min) IFNγ treatment condition. Protein complexes were eluted from the beads using 42 μl of lane marker reducing sample buffer. 40 μl of each sample were submitted for nano-liquid chromatography-tandem mass spectrometry analysis and 2 μl were resolved by SDS-PAGE and immunoblotted to assess ULK1 expression for each experimental condition using a primary anti-ULK1 rabbit antibody and a mouse anti-rabbit IgG light chain specific HRP-conjugated secondary antibody, as shown in B.

Supplementary Figure S6

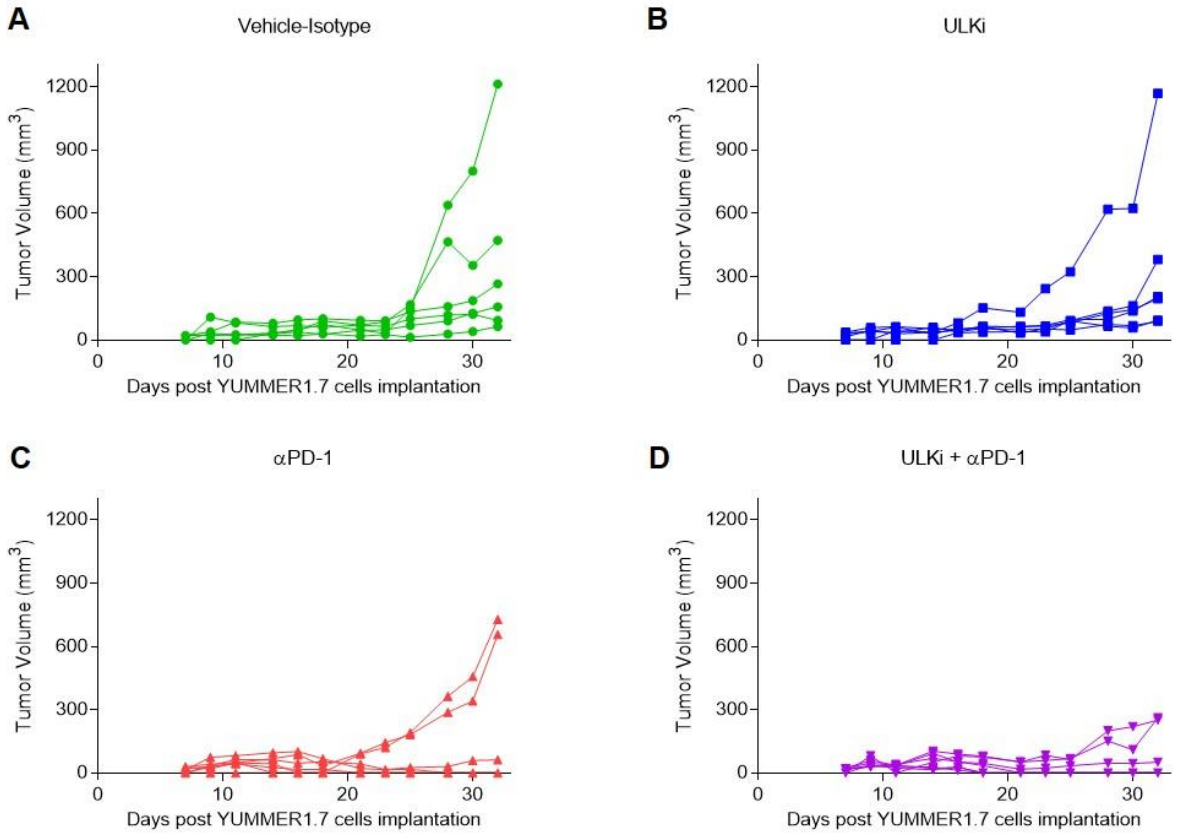

Supplementary Figure S6. Pharmacological inhibition of ULK1 enhances the anti-tumor effects of anti-PD-1 therapy in YUMMER1.7 mouse melanoma *in vivo* model. YUMMER1.7 tumor-bearing mice were treated as detailed in Figure 5A. (A-D) Tumor volume was measured three times per week throughout the study. Each line represents data for an individual mouse per treatment group (n = 6 for vehicle-isotype and ULKi, n = 7 for αPD-1 and ULKi + αPD-1 treatment groups). Results are representative of two independent *in vivo* studies.

Supplementary Figure S7

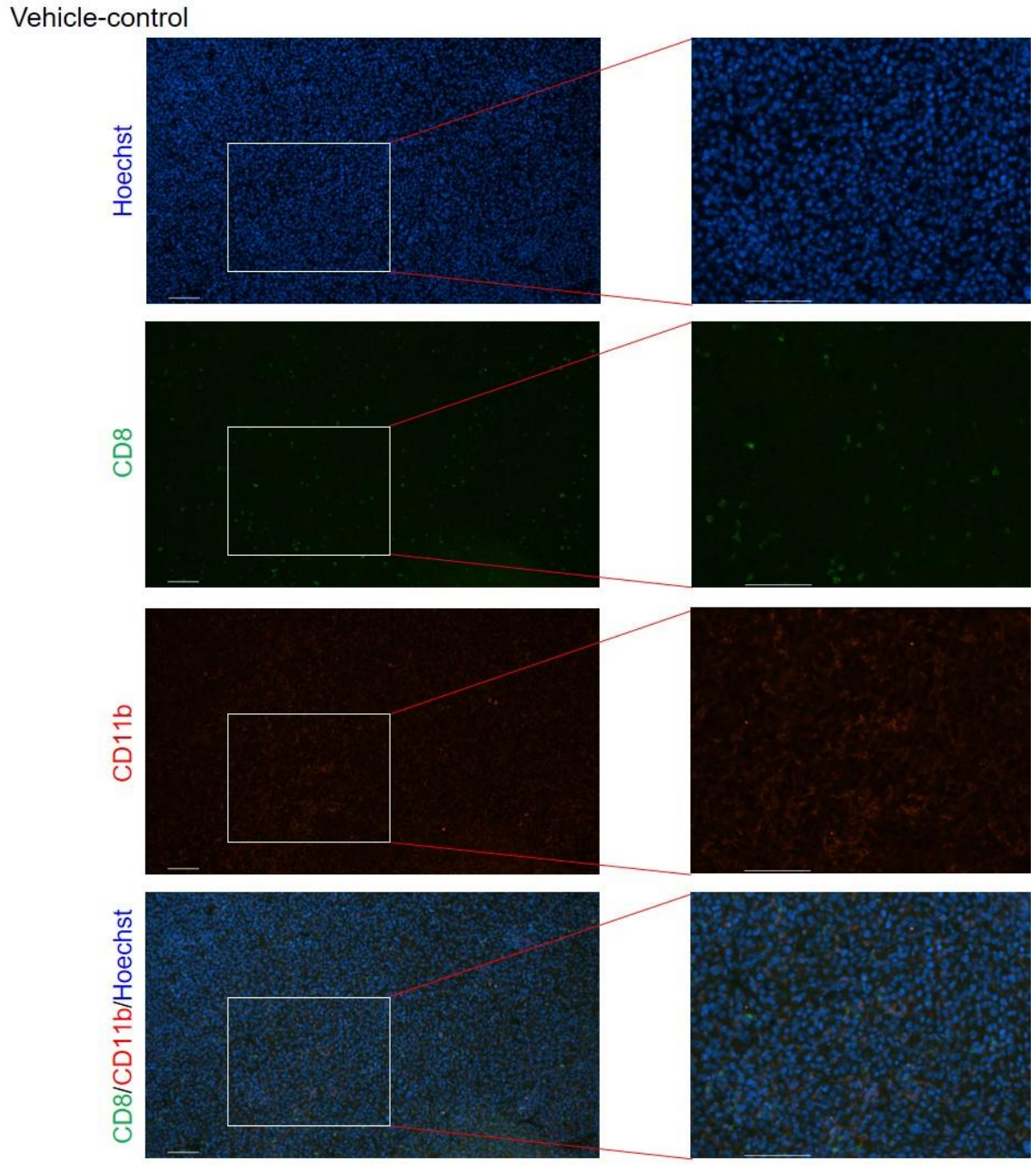

Supplementary Figure S7. Tumor infiltrating CD8⁺ T cells and TAMCs in vehicle-isotype-treated mice. Representative immunofluorescence images of CD8⁺ T cells (CD8) and TAMCs (CD11b) in tumors isolated from mice treated with vehicle-isotype. Pictures were taken with Nikon Ti2 Widefield microscope equipped with Photometrics IRIS15 sCMOS camera with a 10X panfluorNA03 objective and analyzed using NIS Elements Imaging software. See also figure 6A.

Supplementary Figure S8

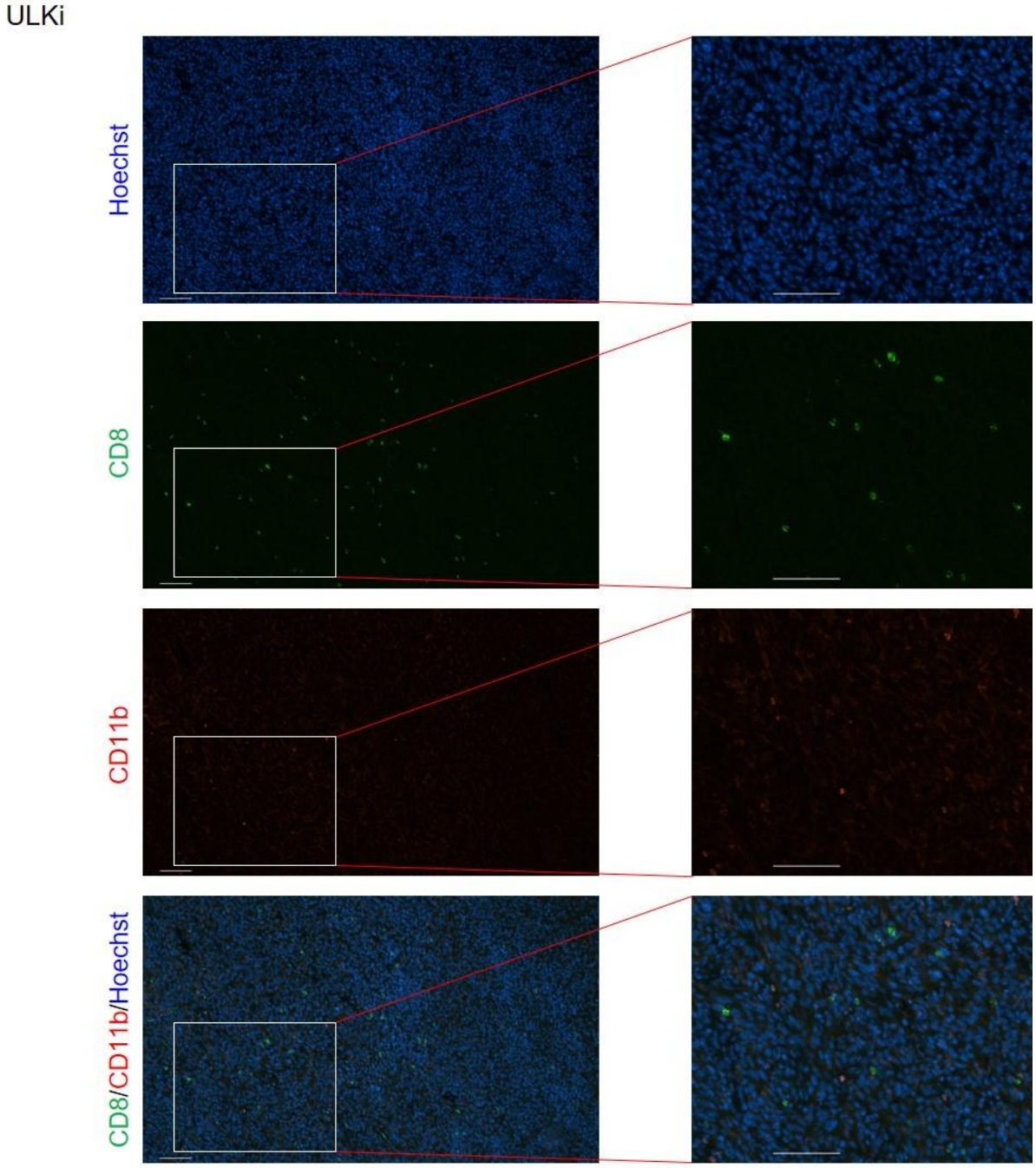

Supplementary Figure S8. Tumor infiltrating CD8$^+$ T cells and TAMCs in ULK inhibitor-treated mice. Representative immunofluorescence images of CD8$^+$ T cells (CD8) and TAMCs (CD11b) in tumors isolated from mice treated with ULK inhibitor (ULKi). Pictures were taken with Nikon Ti2 Widefield microscope equipped with Photometrics IRIS15 sCMOS camera with a 10X panfluorNA03 objective and analyzed using NIS Elements Imaging software. See also figure 6A.

Supplementary Figure S9

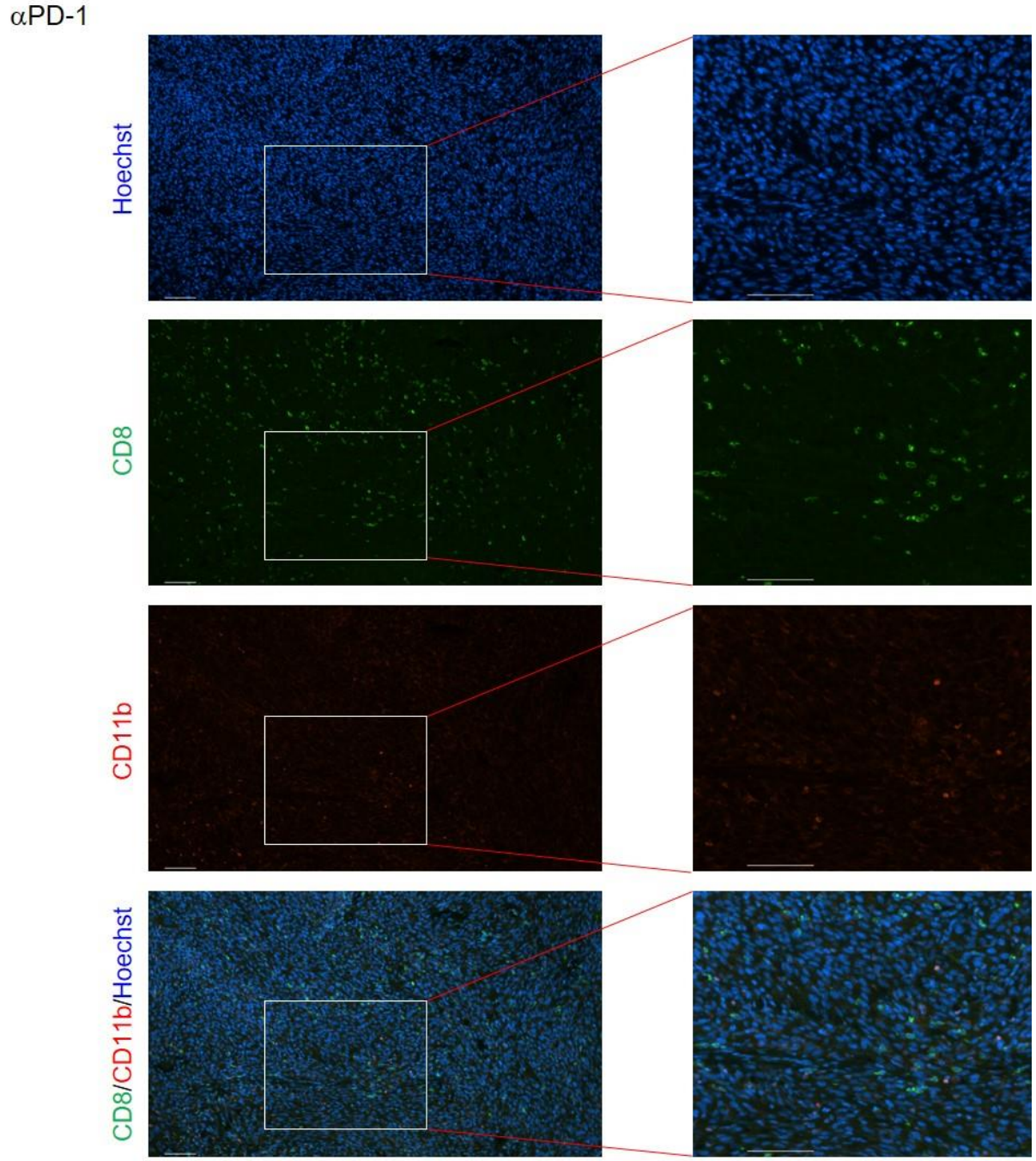

Supplementary Figure S9. Tumor infiltrating CD8⁺ T cells and TAMCs in anti-PD-1-treated mice. Representative immunofluorescence images of CD8⁺ T cells (CD8) and TAMCs (CD11b) in tumors isolated from mice treated with anti-PD-1. Pictures were taken with Nikon Ti2 Widefield microscope equipped with Photometrics IRIS15 sCMOS camera with a 10X panfluorNA03 objective and analyzed using NIS Elements Imaging software. See also figure 6A.

Supplementary Figure S10

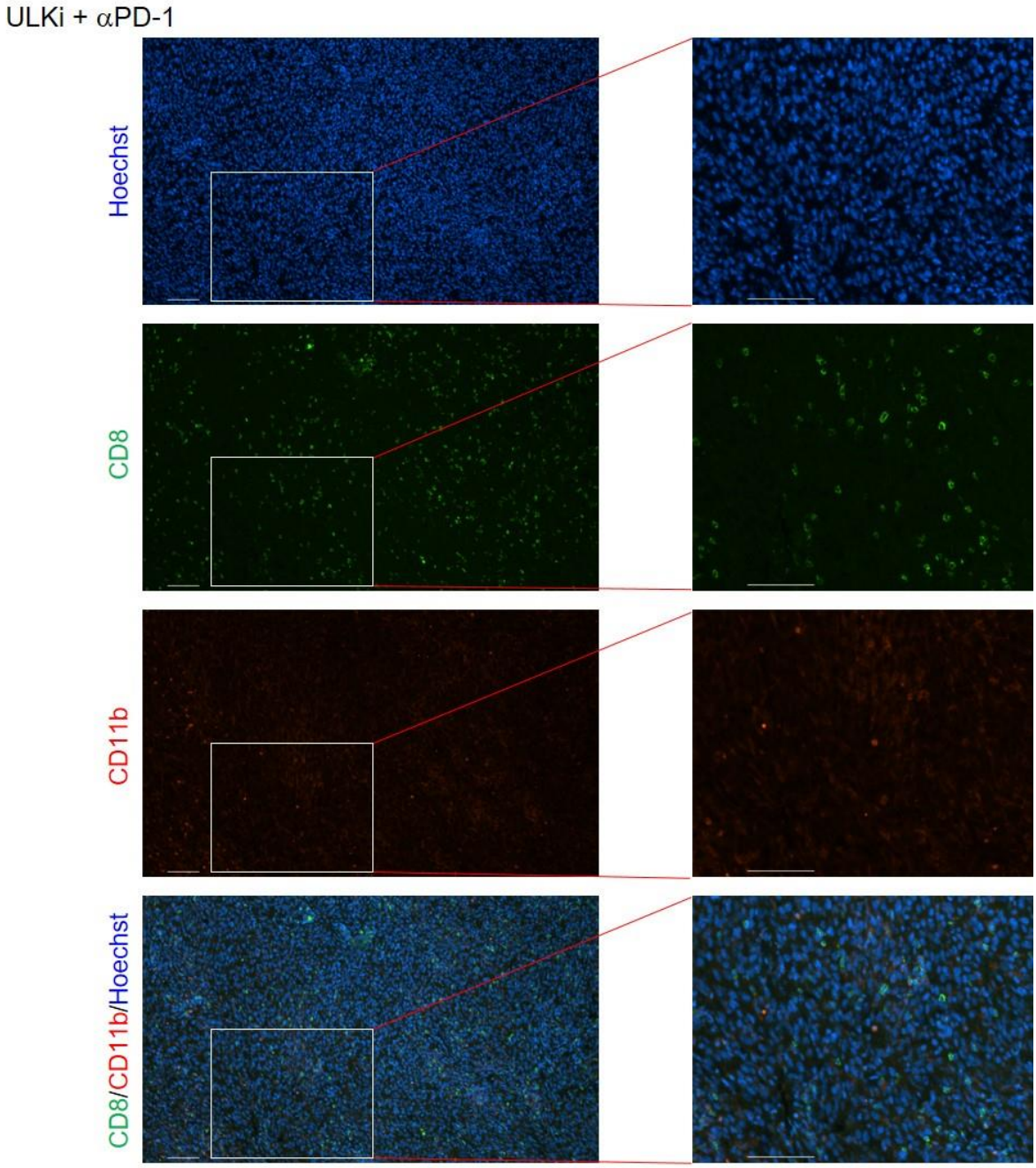

Supplementary Figure S10. Tumor infiltrating CD8$^+$ T cells and TAMCs in ULKi plus anti-PD-1-treated mice. Representative immunofluorescence images of CD8$^+$ T cells (CD8) and TAMCs (CD11b) in tumors isolated from mice treated with ULKi + anti-PD-1. Pictures were taken with Nikon Ti2 Widefield microscope equipped with Photometrics IRIS15 sCMOS camera with a 10X panfluorNA03 objective and analyzed using NIS Elements Imaging software. See also figure 6A.

Supplementary Figure S11

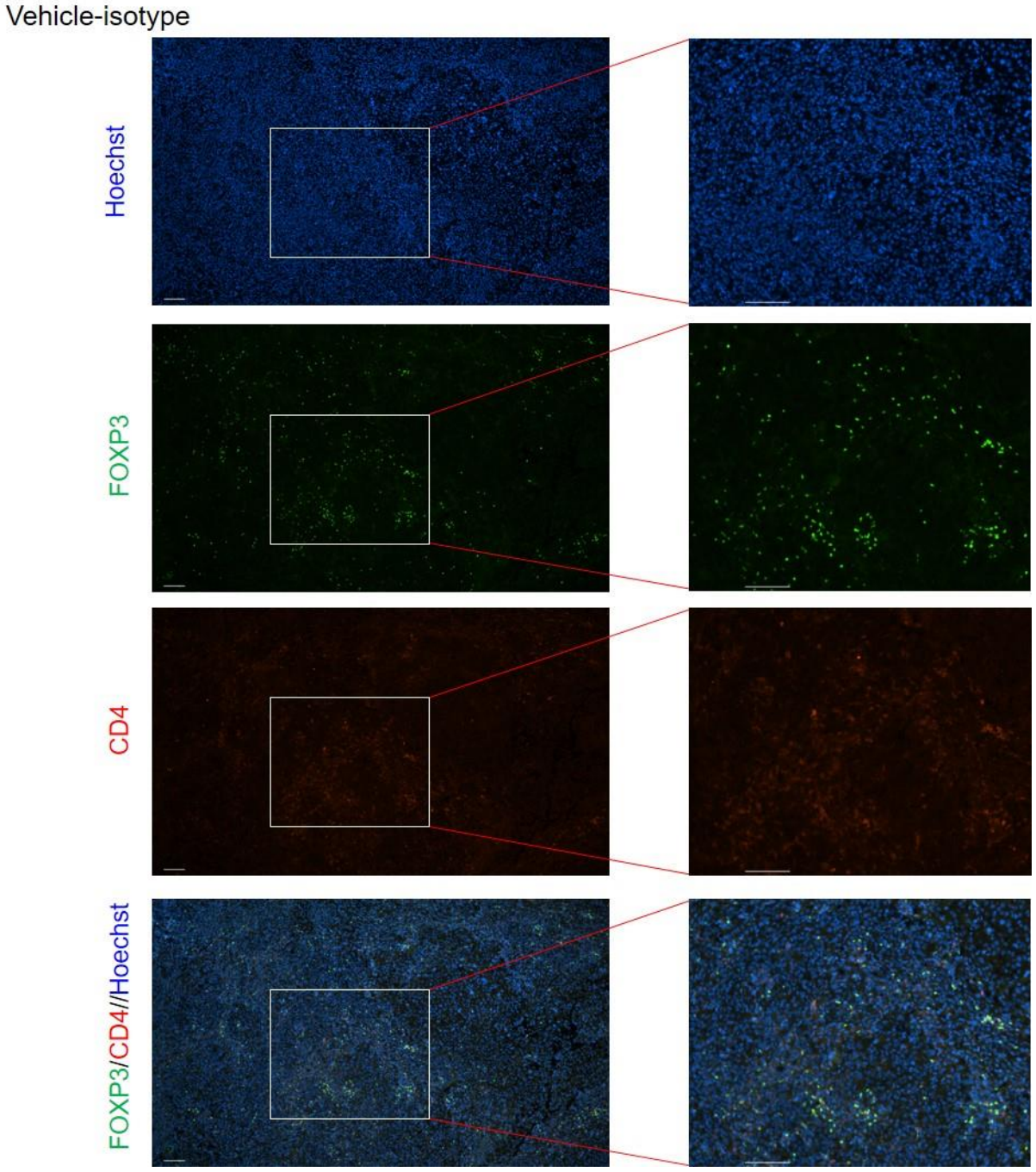

Supplementary Figure S11. Tumor infiltrating CD4⁺ T cells and Tregs in vehicle-isotype-treated mice. Representative immunofluorescence images of CD4⁺ T cells (CD4) and Tregs (FOXP3) in tumors isolated from mice treated with vehicle-isotype. Pictures were taken with Nikon Ti2 Widefield microscope equipped with Photometrics IRIS15 sCMOS camera with a 10X panfluorNA03 objective and analyzed using NIS Elements Imaging software. See also figure 6A.

Supplementary Figure S12

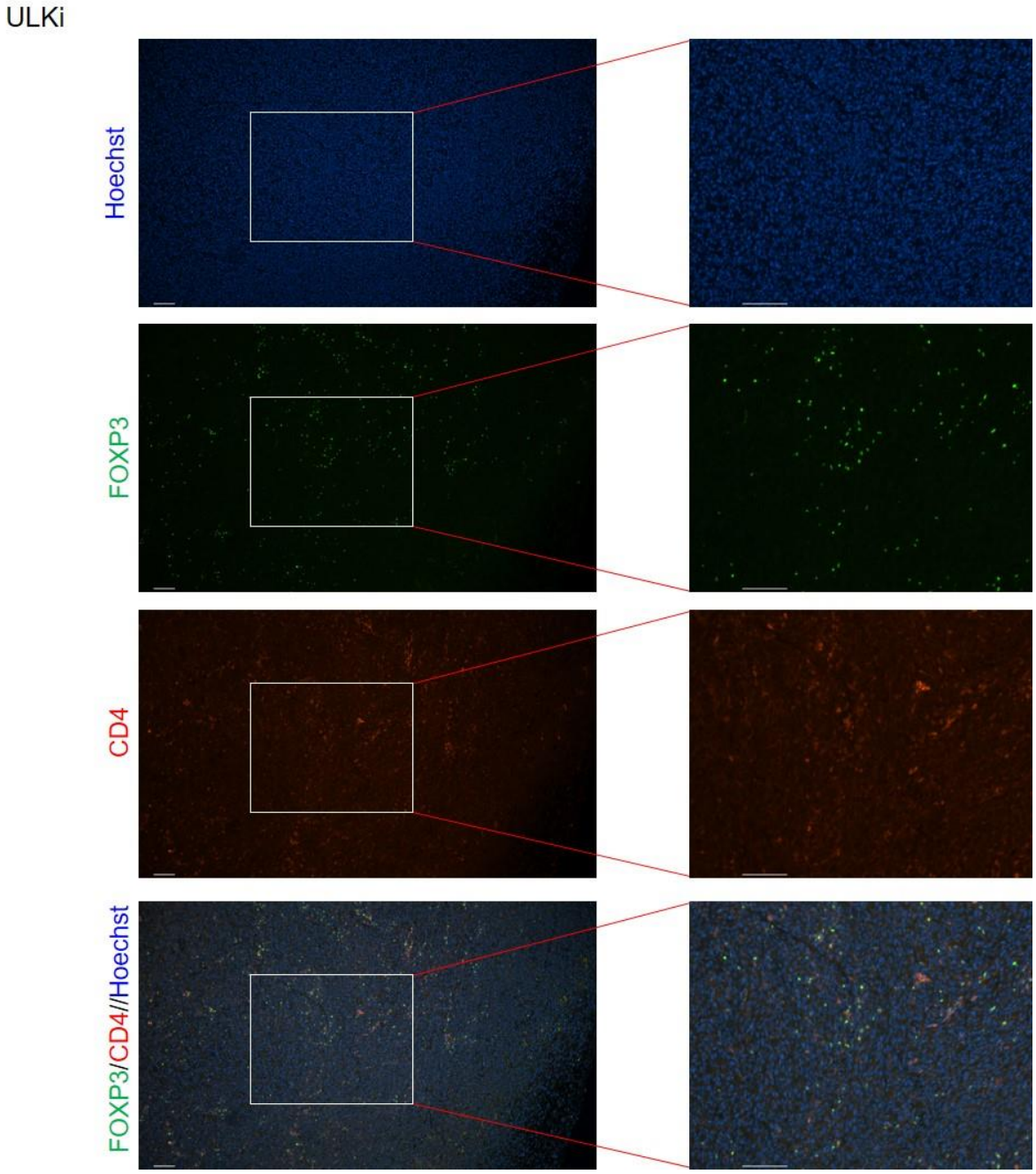

Supplementary Figure S12. Tumor infiltrating CD4⁺ T cells and Tregs in ULK inhibitor-treated mice. Representative immunofluorescence images of CD4⁺ T cells (CD4) and Tregs (FOXP3) in tumors isolated from mice treated with ULKi. Pictures were taken with Nikon Ti2 Widefield microscope equipped with Photometrics IRIS15 sCMOS camera with a 10X panfluorNA03 objective and analyzed using NIS Elements Imaging software. See also figure 6A.

Supplementary Figure S13

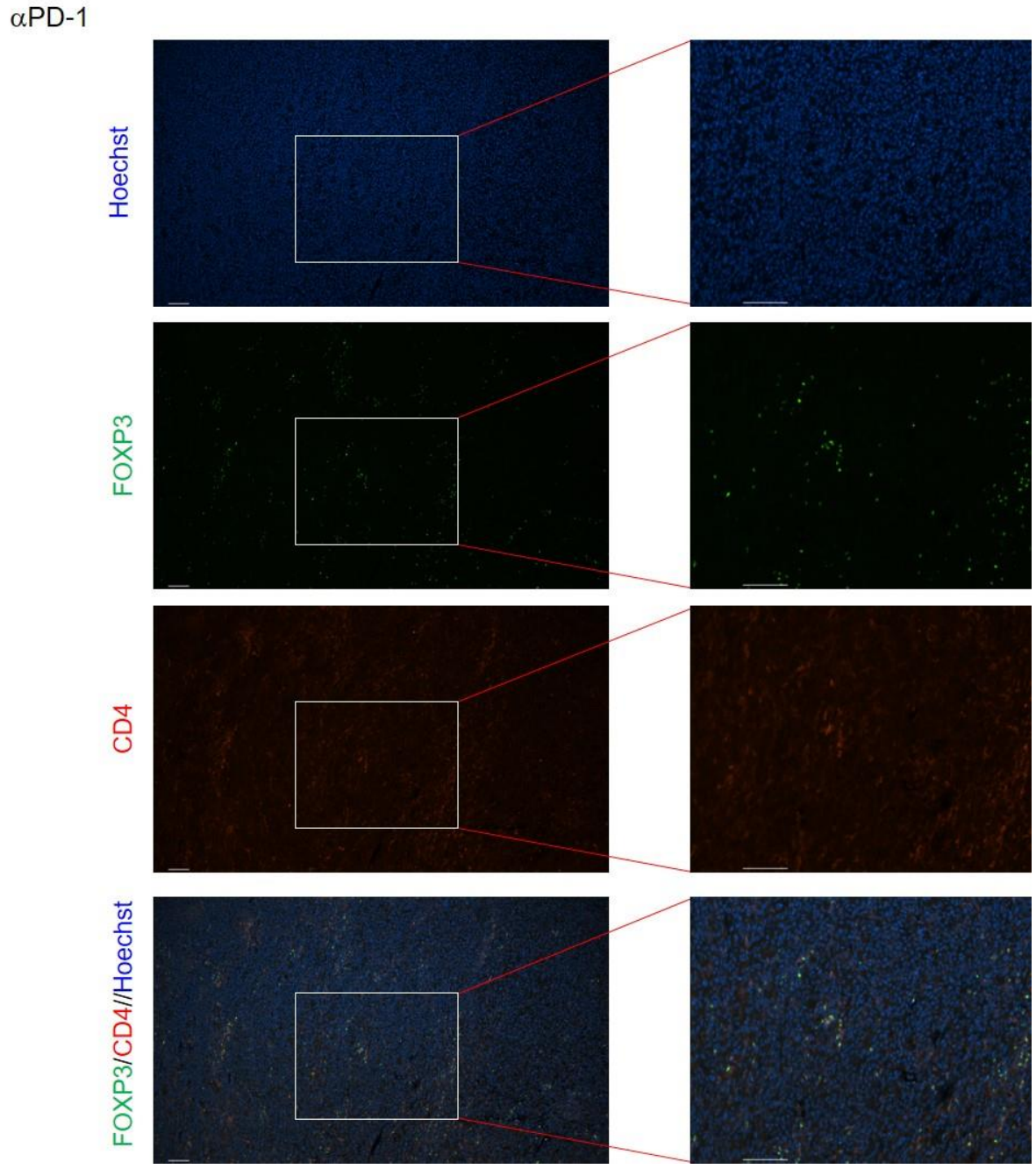

Supplementary Figure S13. Tumor infiltrating CD4⁺ T cells and Tregs in anti-PD-1-treated mice. Representative immunofluorescence images of CD4⁺ T cells (CD4) and Tregs (FOXP3) in tumors isolated from mice treated with anti-PD-1. Pictures were taken with Nikon Ti2 Widefield microscope equipped with Photometrics IRIS15 sCMOS camera with a 10X panfluorNA03 objective and analyzed using NIS Elements Imaging software. See also figure 6A.

Supplementary Figure S14

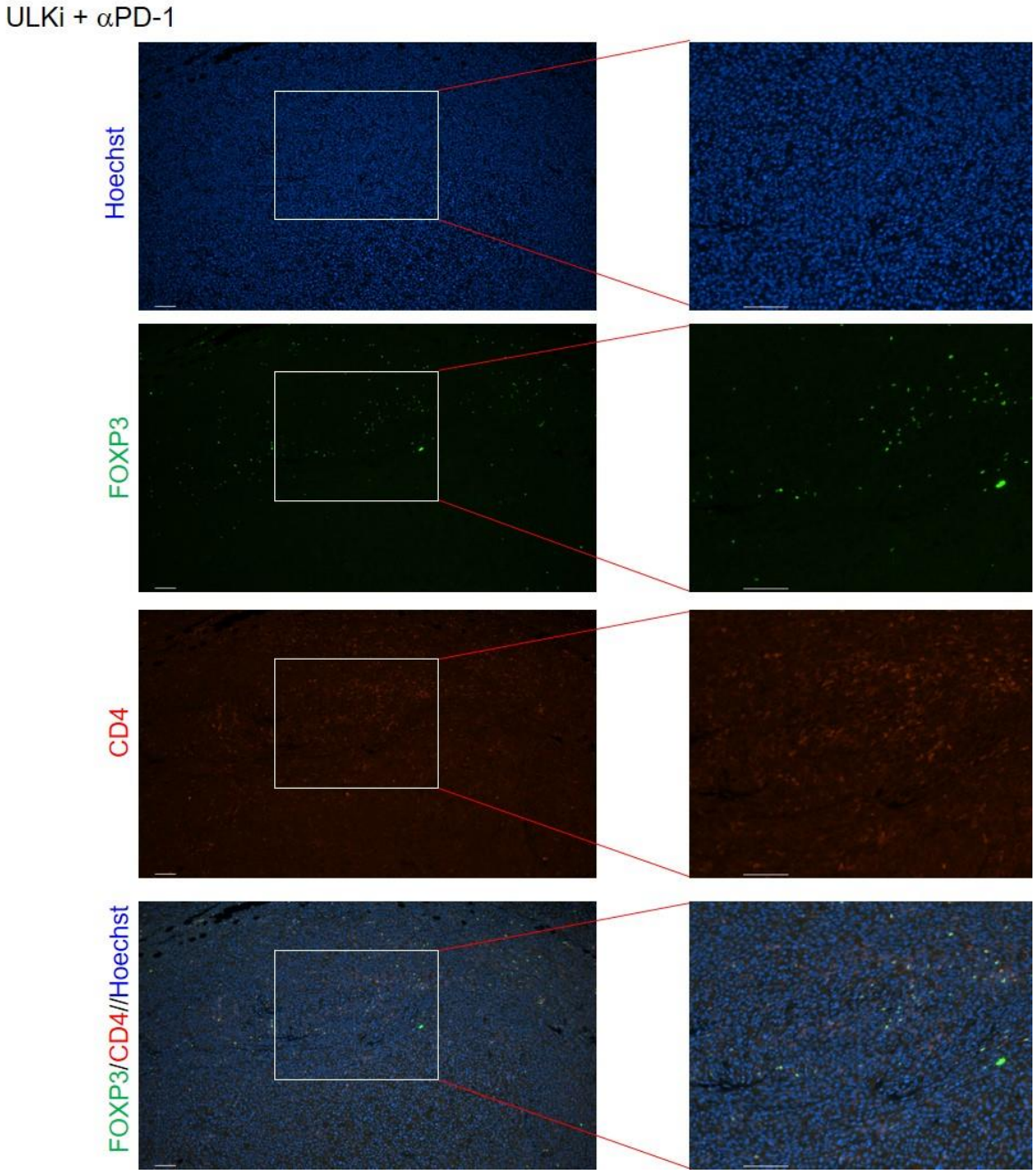

Supplementary Figure S14. Tumor infiltrating CD4⁺ T cells and Tregs in ULKi plus anti-PD-1-treated mice. Representative immunofluorescence images of CD4⁺ T cells (CD4) and Tregs (FOXP3) in tumors isolated from mice treated with ULKi + anti-PD-1. Pictures were taken with Nikon Ti2 Widefield microscope equipped with Photometrics IRIS15 sCMOS camera with a 10X panfluorNA03 objective and analyzed using NIS Elements Imaging software. See also figure 6A.

Supplementary Figure S15

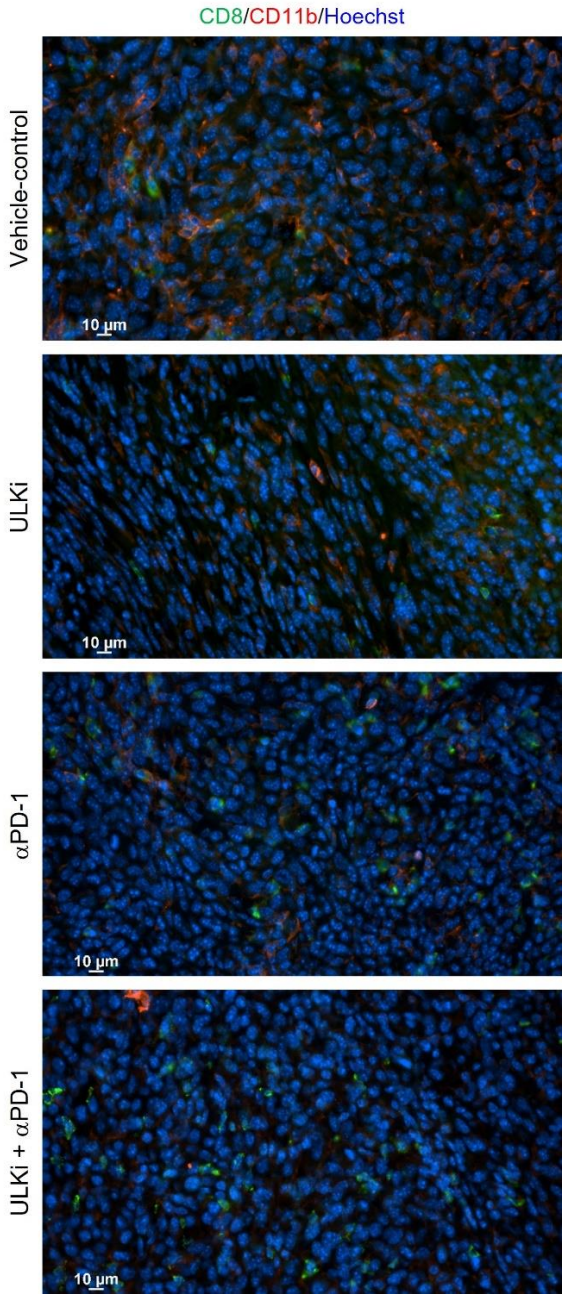

Supplementary Figure S15. Tumor infiltrating CD8$^+$ T cells and TAMCs in control, ULKi and/or anti-PD-1-treated mice. Representative immunofluorescence images of CD8$^+$ T cells (CD8) and TAMCs (CD11b) in tumors isolated from mice treated with either vehicle-isotype, ULKi, and/or anti-PD-1. Pictures were taken with Nikon Ti2 Widefield microscope equipped with Photometrics IRIS15 sCMOS camera with a 40X SPanfluorNA06 objective and analyzed using NIS Elements Imaging software. See also figure 6A.

Supplementary Figure S16

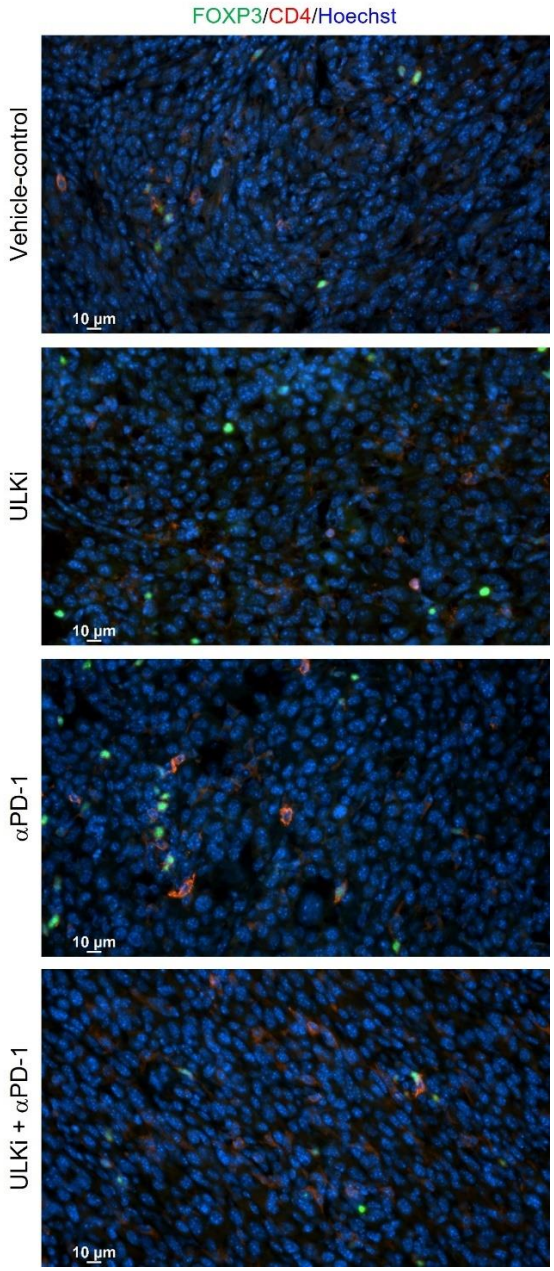

Supplementary Figure S16. Tumor infiltrating CD4$^+$ T cells and Tregs in control, ULKi and/or anti-PD-1-treated mice. Representative immunofluorescence images of CD4$^+$ T cells (CD4) and Tregs (FOXP3) in tumors isolated from mice treated with either vehicle-isotype, ULKi, and/or anti-PD-1. Pictures were taken with Nikon Ti2 Widefield microscope equipped with Photometrics IRIS15 sCMOS camera with a 40X SPanfluorNA06 objective and analyzed using NIS Elements Imaging software. See also figure 6A.

Supplementary Figure S17

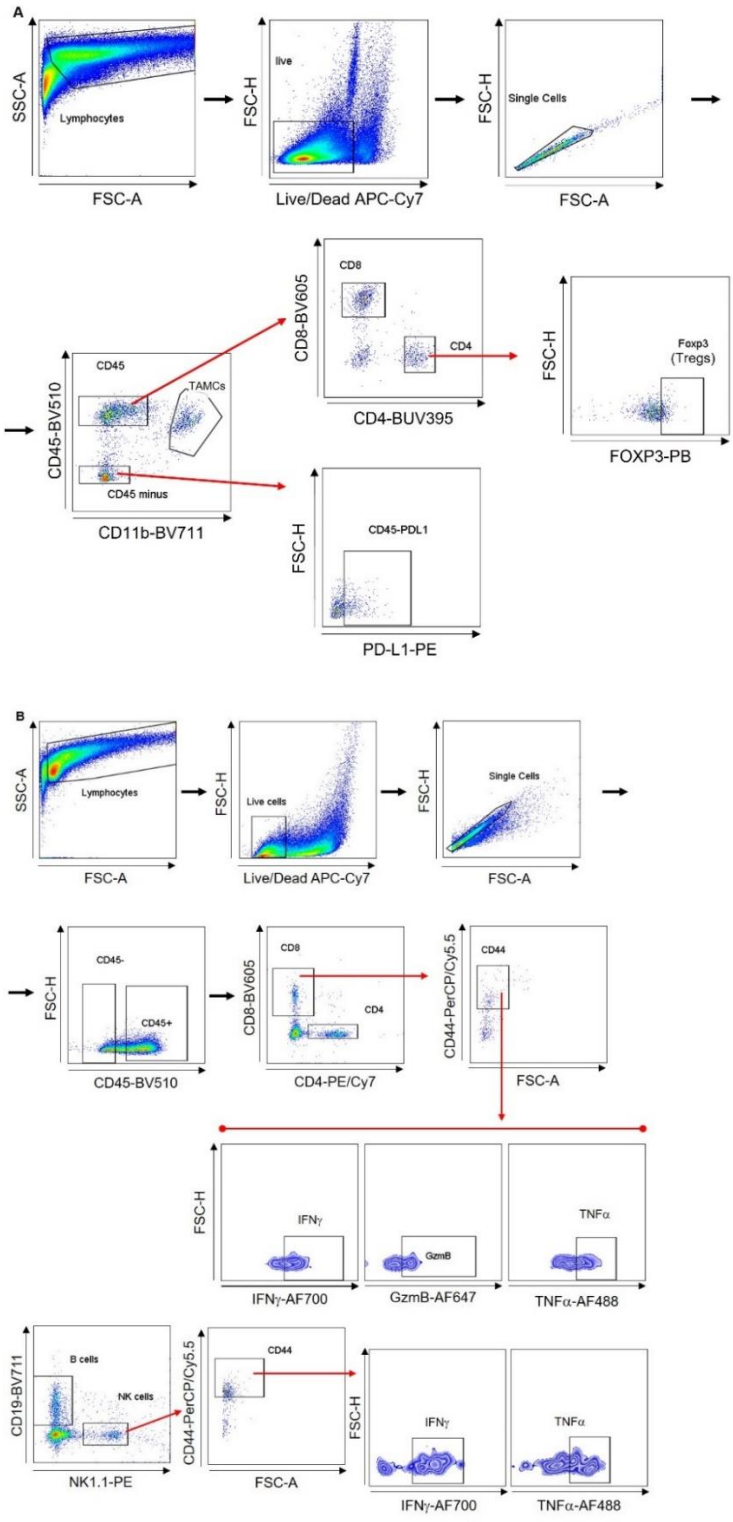

Supplementary Figure S17. Gating strategy for flow cytometric immunophenotyping of mouse melanoma tumors. (A) Representative images of the flow cytometry gating strategy used to assess

the percentage of CD45 negative PD-L1+ cells, CD8+ T cells, CD4+ T cells, Tregs and TAMCs in YUMMER1.7 melanoma tumors shown in Figures 5G, 6B-D and 6M using anti- CD45-BV510, CD11b-BV711, CD8-BV605, CD4-BUV395, FOXP3-pacific blue (PB) and PD-L1-PE antibodies. (B) Representative images of the flow cytometry gating strategy used to assess the percentage of active CD8+ T cells expressing IFNγ, granzyme B (GzmB) and TNFα, and the percentage of active NK cells expressing IFNγ and TNFα in YUMMER1.7 melanoma tumors shown in Figures 6G-L using anti-CD45-BV510, CD8 BV605, CD4-PE/Cy7, CD44-PercPCy5.5, NK-1.1-PE, IFNγ-AF700, GzmB-AF647, and TNFα-AF488 antibodies.

Supplementary Materials and Methods

Quantitative RT-PCR analysis

Total RNA was isolated from *in vitro* treated melanoma cells or *in vivo* treated YUMMER1.7 mouse tumors after homogenization using the RNeasy Mini Kit (QIAGEN) following the manufacturer's instructions. One to two micrograms of total cellular mRNA were reverse-transcribed into cDNA using the High Capacity cDNA Reverse Transcription Kit (Applied Biosystems). Quantitative RT-PCR was performed using a Bio-Rad CFX96 Real Time System (Bio-Rad) and fluorescein amidite (FAM)-labeled primer/probe sets (Thermo Fisher Scientific). mRNA expression was determined for human *ULK1* (Hs00177504_m1), *PD-L1* (*CD274*, Hs00204257_m1), *PD-L2* (*PDCD1LG2*, Hs00228839_m1), *HLA-B* (Hs00818803_g1), *IFI30* (Hs00173838_m1), *TAP1* (Hs00388675_m1) and *STAT1* (Hs01013996_m1). mRNA expression was also determined for mouse *Pd-l1* (*Cd274*, Mm03048248_m1), *Pd-l2* (*Pdcd1lg2*, Mm00451734_m1) *Stat1* (Mm01257286_m1) and *Tap1* (Mm00443188_m1). Human *GAPDH* (Hs02758991_g1) or mouse *Gapdh* (Mm99999915_g1) expression were used as reference genes. Bio-Rad CFX Maestro software was used to collect Ct values. Delta Ct (ΔCt) was calculated for each gene and the ΔΔCt method was used to calculate mRNA expression for each experimental condition. Data are presented as the increase or decrease in fold change compared to the control group or control sample.

Immunoblotting analysis

Cell pellets were lysed in protein lysis buffer [50 mM Hepes (pH 7.3), 150 mM NaCl, 1.5 mM MgCl2, 1 mM EDTA (pH 8.0), 100 µM sodium fluoride, 10 µM sodium pyrophosphate, 0.5% Triton X-100, and 10% glycerol] supplemented with protease and phosphatase inhibitors, and processed for immunoblotting analyses as previously reported (1). Membranes were probed with primary antibodies against: STAT1 (1:1000, clone E-23, Santa Cruz Biotechnology #sc-346, RRID:AB_632435), human IDO1 (1:1000, clone D5J4E, Cell Signaling Technology # 86630,

RRID:AB_2636818), mouse IDO1 (1:1000, clone D7Z7U, Cell Signaling Technology #68572, RRID:AB_2799750), ULK1 (1:1000, clone D8H5, Cell Signaling Technology #8054, RRID:AB_11178668), IRF1 (1:1000, clone D5E4, Cell Signaling Technology #8478, RRID:AB_10949108), Lamin A/C (1:1000, Cell Signaling Technology #2032, RRID:AB_2136278), β-Tubulin (1:1000, clone D3U1W, Cell Signaling Technology #86298, RRID:AB_2715541) and GAPDH (1:20,000, clone 6C5, EMD Millipore #MAB374, RRID:AB_2107445).

Cytoplasmic and nuclear cell fractionation

Cytoplasmic and nuclear cell fractionation was performed using the NE-PER Nuclear and Cytoplasmic Extraction Reagent Kit (Thermo Fisher Scientific #78835), according to manufacturer's instructions. Cytoplasmic and nuclear cell lysates were then processed for immunoblotting analysis or for co-immunoprecipitation of ULK1-protein complexes followed by either mass spectrometry analysis or immunoblotting analysis.

Co-immunoprecipitation of ULK1-protein complexes

For mass spectrometry analysis, 1750 μg of nuclear cell lysates and 2800 μg of cytoplasmic cell lysates from each treatment condition were used for co-immunoprecipitation (co-IP) of endogenous ULK1-protein complexes. Cell lysates were incubated overnight at 4°C with rotation with ULK1 (D8H5) rabbit monoclonal antibody conjugated to sepharose beads (20 µl/mg nuclear proteins and 15 µl/mg cytosolic proteins) (Cell Signaling Technology, custom order). As negative control, the same procedure was followed using rabbit (DA1E) monoclonal antibody IgG XP Isotype control conjugated to sepharose beads (Cell Signaling Technology #3423, RRID:AB_1550040) instead of ULK1 antibody. For immunoblotting analysis of ULK1-IRF1 interaction, 750 μg of nuclear and/or cytoplasmic lysates were incubated overnight at 4°C with

rotation with ULK1 (D8H5) rabbit monoclonal antibody (2.9 µg/mg protein, Cell Signaling Technology #8054, RRID:AB_11178668), followed by incubation for 1 h at 4 °C with rotation with protein G Sepharose 4 Fast Flow beads (GE Healthcare). As control, the same procedure was followed using rabbit (DA1E) monoclonal antibody IgG XP Isotype control (Cell Signaling Technology #3900, RRID:AB_1550038) instead of ULK1 antibody. After co-IP, the beads were washed three times with NP-40 lysis buffer (20 mM Hepes pH 7.4, 180 mM KCl, 0.2 mM EGTA and 0.1% NP-40). Protein-ULK1 complexes were eluted from the beads by incubation with Lane Marker Reducing Sample Buffer (Pierce) at 95°C for 10 minutes. Eluates were either submitted for mass spectrometry analysis or resolved by SDS-PAGE and processed for immunoblotting analyses.

Mass spectrometry analysis

Mass spectroscopy analysis was performed by the Northwestern Proteomics Core Facility (Northwestern University, Chicago) as previously described (1). The mass spectrometry proteomics data generated in this study have been deposited to the ProteomeXchange Consortium via the PRIDE (2) partner repository with the project accession #: PXD035347.

Chromatin-immunoprecipitation assay

For the chromatin immunoprecipitation (ChIP) assay, A375 cells were pre-treated with either vehicle-control (DMSO) or 10μM SBI for 1 hour, followed by 6 hours treatment with either vehicle-control (DMSO), 10μM SBI and/or 2,500 IU/mL IFNγ. ChIP assay was performed as previously reported (3) using the SimpleChIP Enzymatic Chromatin IP Kit with Magnetic Beads (Cell Signaling) per manufacturer's instructions. Anti-IRF1 antibody (Proteintech, #11335-1-AP, RRID:AB_2877759) was used for IP of IRF1 and normal rabbit IgG (Cell Signaling Technology #2729, RRID:AB_1031062) was used as negative control. Quantitative RT-PCR was performed

on purified immunoprecipitated DNA for the PD-L1 promoter IRF1 binding site, HLA-B promoter IRF1 binding site and RPL30 promoter as a negative control using SsoAdvanced Universal SYBR Green supermix following manufacturer's guidelines with previously published primers (4):

PDL1 FWD-GCTTTAATCTTCGAAACTCTTCCC,

PDL1 REV-CCTAGGAATAAAGCTGTGTATAGAAATG,

HLA-B FWD-GAGTTTCACTTCTTCTCCCAACCT,

HLA-B REV-GGACGCGTCACGAGTATCCT

and SimpleChIP Human RPL30 Exon 3 Primers (Cell Signaling Technology #7014). All quantitative RT-PCR signals were normalized to the input DNA.

Flow cytometric immunophenotyping of mouse melanoma tumors

Mouse tumor single-cell suspensions were prepared for flow cytometric immunophenotypic analysis as previously described (5). Cells were incubated with Fc receptor blocking antibody (anti-CD16/32 clone 93, BioLegend #101301, RRID:AB_312800) in FACS buffer (2% FBS in PBS) for 20 minutes at 4°C followed by staining with antibodies against surface markers. Next, fixable viability dye eFluor780 (Thermo Fisher Scientific # 65-0865-14) was used to stain live cells in PBS. For intracellular staining, cells were first fixed and permeabilized using eBioscience Foxp3/Transcription Factor Staining Buffer Set (Invitrogen, Thermo Fisher Scientific #00-5523-00), according to manufacturer's protocol. For cytokine staining, cells were preincubated with phorbol 12-myristate 13-acetate (PMA)/ionomycin + brefeldin A for 4 hours before staining. The following antibodies were used for tumor, myeloid and lymphocytic analysis: Brilliant Violet 510 anti-mouse CD45 clone 30-F11 (BioLegend #103138, RRID:AB_2563061), Brilliant Violet 605 anti-mouse CD8a clone 53-6.7 (BioLegend #100743, RRID:AB_2561352), Brilliant Violet 711 anti-mouse/human CD11b clone M1/70 (BioLegend #101241, RRID:AB_11218791), PE anti-mouse CD274 (B7-H1, PD-L1) clone 10F.9G2 (BioLegend #124308, RRID:AB_2073556), PE/Cyanine7 anti-mouse NK-1.1 clone PK136 (BioLegend

#108714, RRID:AB_389364), BUV395 rat anti-mouse CD4 clone GK1.5 (BD Biosciences #563790, RRID:AB_2738426) and Pacific Blue anti-mouse FOXP3 clone MF-14 (BioLegend #126409, RRID:AB_2247064). The following antibodies were used for cytokine analysis: PerCP/Cyanine5.5 anti-mouse/human CD44 clone IM7 (BioLegend #103031, RRID:AB_2076206), Brilliant Violet 510 anti-mouse CD45 clone 30-F11 (BioLegend #103138, RRID:AB_2563061), Brilliant Violet 605 anti-mouse CD8a clone 53-6.7 (BioLegend #100743, RRID:AB_2561352), PE anti-mouse NK-1.1 clone PK136 (BioLegend #108707, RRID:AB_313394), PE/Cyanine7 anti-mouse CD4 clone RM4-5 (BioLegend #100528, RRID:AB_312729), Alexa Fluor 488 anti-mouse TNF-α clone MP6-XT22 (BioLegend #506313, RRID:AB_493328), Alexa Fluor 647 anti-human/mouse Granzyme B clone GB11 (BioLegend #515405, RRID:AB_2294995) and Alexa Fluor 700 anti-mouse IFN-γ clone XMG1.2 (BioLegend #505824, RRID:AB_2561300). All antibodies were used at a 1:100 dilution in FACS buffer and cells were stained for 30 minutes at 4°C. Unstained and single-color controls were used for each experiment using fresh splenocytes isolated from naïve C57BL/6 mice and to perform compensation. OneComp eBeads (Invitrogen #01-1111-42) were also used for single-color compensation to create/confirm multi-color compensation matrices. These experiments were performed without including fluorescence minus one and isotype controls. Data were acquired with BD FACS Symphony flow cytometer and analyzed using FlowJo (RRID:SCR_008520) v10.6 software.

Immunofluorescence staining of mouse melanoma tumors

For immune cell detection in YUMMER1.7 tumors, formalin-fixed paraffin-embedded tissue sections (4 μm thick) from the mouse tumors were first incubated with sodium citrate buffer (pH = 6) at 110°C for 20 minutes in a pressure cooker for antigen retrieval. Staining was then completed on an automated platform (IntelliPATH by Biocare Medical). Primary antibodies against murine CD8a (4SM16) eBioscience (1:150, Thermo Fisher Scientific #14-0195-82,

RRID:AB_2637159), CD11b (EPR1344) (1:200, Abcam #ab133357, RRID:AB_2650514), FOXP3 (FJK-16s) eBioscience (1:200, Thermo Fisher Scientific #14-5773-82, RRID:AB_467576) and CD4 (EPR19514) (1:200, Abcam #ab183685, RRID:AB_2686917) were used. To detect CD8/CD11b and FOXP3/CD4 expression Biotin-SP (long spacer) AffiniPure Donkey Anti-Rat IgG (H+L) (1:100, Jackson ImmunoResearch, #712-065-153) with an in-house (MHPL) TSA amplification followed by Alexa Fluor 488 Streptavidin (1:500) and Cy3 AffiniPure Donkey Anti-Rabbit IgG (H+L) (1:500, Jackson ImmunoResearch, #711-165-152) were used. Mounting was performed using Fluor shield with Hoechst (Sigma). Images were taken with a Nikon Ti2 Widefield microscope equipped with Photometrics IRIS15 sCMOS camera with a 10X panfluorNA03 objective and a 40X SPanfluorNA06 objective. Data was processed using NIS Elements Imaging software (RRID:SCR_014329).

References for Supplementary Materials and Methods

1. Saleiro D, Wen JQ, Kosciuczuk EM, Eckerdt F, Beauchamp EM, Oku CV, et al. Discovery of a signaling feedback circuit that defines interferon responses in myeloproliferative neoplasms. Nat Commun. 2022;13(1):1750.

2. Perez-Riverol Y, Csordas A, Bai J, Bernal-Llinares M, Hewapathirana S, Kundu DJ, et al. The PRIDE database and related tools and resources in 2019: improving support for quantification data. Nucleic Acids Res. 2019;47(D1):D442-D450.

3. Fischietti M, Eckerdt F, Blyth GT, Arslan AD, Mati WM, Oku CV, et al. Schlafen 5 as a novel therapeutic target in pancreatic ductal adenocarcinoma. Oncogene. 2021;40(18):3273-3286.

4. Garcia-Diaz A, Shin DS, Moreno BH, Saco J, Escuin-Ordinas H, Rodriguez GA, et al. Interferon Receptor Signaling Pathways Regulating PD-L1 and PD-L2 Expression. Cell Rep. 2017;19(6):1189-1201.

5. Miska J, Lui JB, Toomer KH, Devarajan P, Cai X, Houghton J, et al. Initiation of inflammatory tumorigenesis by CTLA4 insufficiency due to type 2 cytokines. J Exp Med. 2018;215(3):841-858.